

Topological Transition in Aqueous Nonionic Micellar Solutions

Su Yong Kwon and Mahn Won Kim*

*Department of Physics, Korea Advanced Institute of Science and Technology,
373-1, Gusong-dong, Yusong-gu, Daejeon, 305-701, Korea*
(Received 16 May 2002; published 5 December 2002)

We have studied the topological transition of the nonionic micelles of a penta-ethyleneglycol mono *n*-dodecyl ether ($C_{12}E_5$)/DL- α -phosphatidylcholine Dimyristoyl (DMPC) mixture in water by light scattering and viscosity measurements. The topological transition concentration decreases with an increase of the mixing ratio of DMPC to $C_{12}E_5$. The topological transition point is strongly affected by defect energies of the end cap (ϵ_1) and a threefold junction (ϵ_3) and is compared with a recent theoretical study. This experimental study shows the first clear evidence for the topological transition in a nonionic micellar system resulting from balancing the defect energies.

DOI: 10.1103/PhysRevLett.89.258302

PACS numbers: 82.70.Uv, 78.35.+c, 83.10.Tv, 87.15.Nn

Wormlike or rodlike micelles in aqueous solutions are known to be living polymers and show various phase behaviors as a function of the surfactant concentration. The existence of intermicellar junctions has been of interest since Porte's [1] suggestion for the network of branched wormlike micelles in order to explain the unusual rheological properties of micellar systems in a semidilute regime [2,3]. Since then, the formation of branched cylindrical micelles and their networks has been investigated theoretically [4–7].

Recently Tlustý *et al.* [8] predicted theoretically that the topological transition, from disconnected cylinder to interconnected structure having a threefold junction, is caused by the decreasing spontaneous curvature. The topological transition may be controlled by the tuning of the spontaneous packing geometry (spontaneous curvature), e.g., by changing the temperature, by changing the concentration of added salt in an ionic system, and by adding nonionic additives in nonionic systems. The topological transition gives us good insights into understanding the rheological properties of micellar solutions having junction defects and the phase behaviors of micellar solutions, and also the hierarchical assembly systems, which are characteristics of biological systems [9].

The branched micellar (or microemulsions) structures have been studied mainly by Cryo-TEM. This microscopic technique is a useful tool for direct visualization [10–14], but it does not yield quantitative information on locating the topological transition point. It is difficult to define the transition point as a function of the concentration or temperature by using Cryo-TEM observation. Therefore, no experimental evidence that considers the effect of topological defect (end caps and junctions) energies on the topological transition has been reported until now. Light scattering is a powerful tool to investigate the topological transition points of solutions by measuring the scattering intensity, which responds to different topological structures.

In this Letter, we present the role of topological defects on the topological transition for the first time in aqueous

nonionic micellar solutions using light scattering and viscosity measurements. In our earlier study [15], we reported that the spontaneous curvature of micelles made of $C_{12}E_5$ decreased with the addition of DMPC molecules and the end-cap energy of the micelles increased (Fig. 1). Since mixtures of nonionic surfactants ($C_{12}E_5$) and noncharged phospholipids (DMPC) form mixed micelles with modifying end-cap energy as a function of the molar ratio, m , this is an ideal system to study the effect of defect energies (end-cap-defect energy or junction-defect energy) on the topological transition.

We purchased $C_{12}E_5$ from Nikko Chem. Ltd. (Japan) and the DMPC from Sigma Chem. Corp. The viscosity measurements for the micellar solutions were carried out using a Cannon-Fenske capillary viscometer.

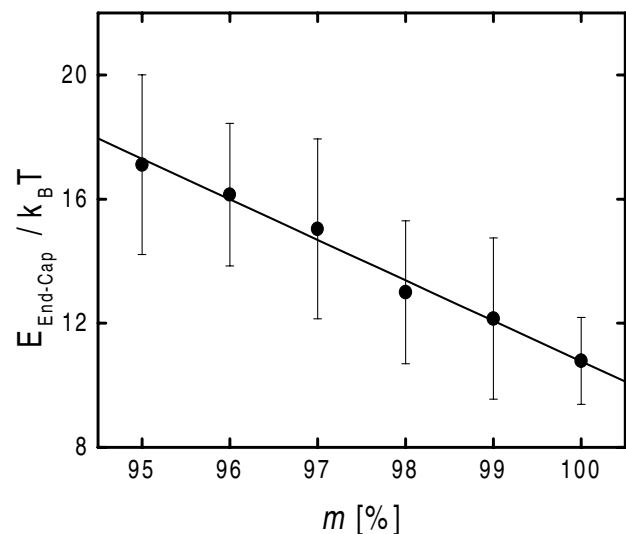


FIG. 1. End-cap energies of $C_{12}E_5$ /DMPC mixed micelle at 288 K. $m = 100$ means a micellar solution made of pure $C_{12}E_5$ and $m = 99$ is a micellar solution made of 99 mole of $C_{12}E_5$ and 1 mole of DMPC. The solid line is a linear fit, which gives the relation $E_{\text{end cap}} \approx -1.29m + 141$ (in units of $k_B T$).

The measured viscosities for the micellar solutions of the $C_{12}E_5$ /DMPC mixture in water are shown in Fig. 2(a). The viscosities increase very slowly at low concentrations; then, above a certain concentration c_J , which presumably corresponds to the crossover from the disconnected cylindrical micelles to the branching of micelles, they increase rapidly. These results can be interpreted as the topological transition [16,17]. We obtained $c_J \sim 2.66 \pm 0.10$, 1.64 ± 0.13 , and 1.15 ± 0.11 mg/ml in 100, 97, and 95 mol%, respectively. Figure 2(b) shows the viscosity with concentration scaled with c_J . All the curves collapse in two regimes, indicating that all samples demonstrate the same topological behavior according to the scaled concentration.

Dynamic light scattering (DLS) and static light scattering (SLS) experiments were made on Brookhaven Instruments using the BI-200SM and the BI9000AT digital correlator at the concentration range of 0.8 to

30 mg/ml in water. Experimental details are described elsewhere [15]. DLS measures the time autocorrelation function of the fluctuations in the scattered light from micelles in solution. This allows determinations of the hydrodynamic radius R_H from the Stokes-Einstein relation,

$$R_H = \frac{k_B T}{6\pi\eta_o D_s}, \quad (1)$$

where k_B and T are, respectively, the Boltzmann constant and the absolute temperature. η_o and D_s are the solvent viscosity and the self-diffusion constant of aggregates, respectively. Figure 3(a) shows the results of R_H as a function of concentration. Again, two growth regimes are identified for all solutions as in the case of the viscosity data in the dilute regime ($c/c_J < 4$). The estimated values of c_J are 2.75 ± 0.20 , 1.55 ± 0.23 , and

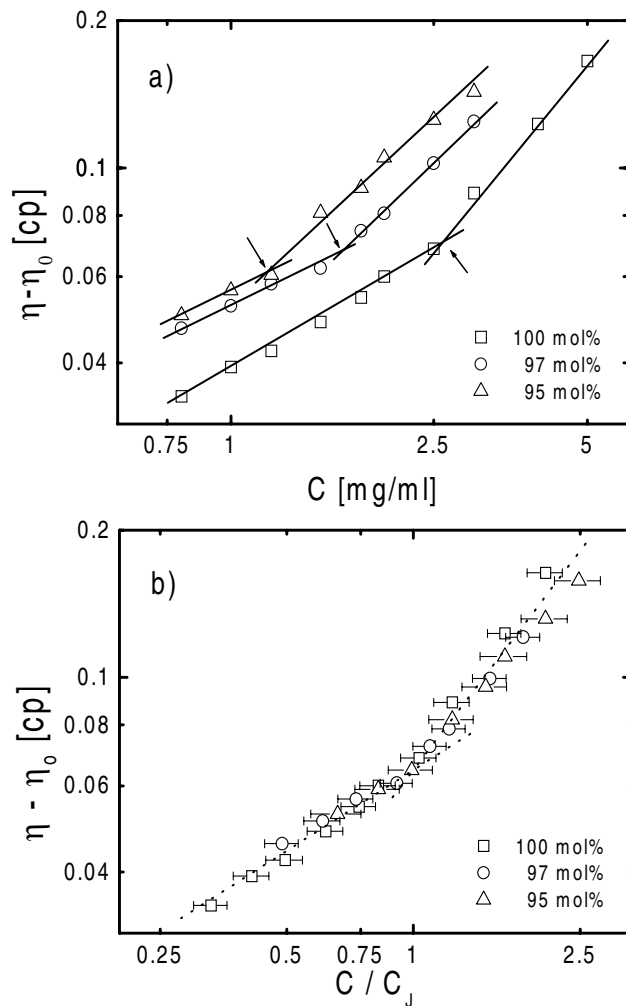


FIG. 2. (a) shows viscosity vs c for three different molar ratios at 288 K and (b) is scaled with c_J , resulting in universal behavior. The solid lines in (a) are linear fits in two regimes and the arrows indicate the transition point, c_J . The dotted line in (b) is meant as a guide to the eye.

258302-2

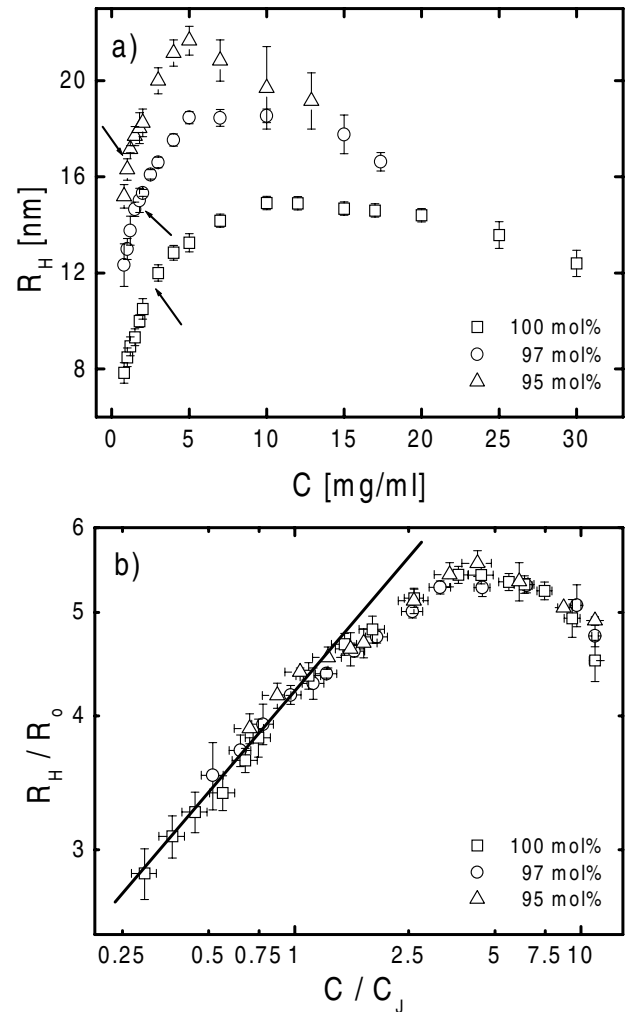


FIG. 3. (a) shows hydrodynamic radius vs c at 288 K and (b) shows the normalized R_H versus c data in units of R_o and c_J , where the R_o is the value of R_H for $c \rightarrow 0$, $R_o \sim 2.7$, 3.5 , and 3.9 nm for 100, 97, and 95 mol%, respectively. The arrows in (a) indicate the transition point, c_J . The solid line in (b) is a linear fit in a log-log plot, which gives the power law $L \sim c^{0.45}$.

258302-2

1.08 ± 0.13 mg/ml for 100, 97, and 95 mol %, respectively, which are consistent with viscosity data. All the curves nicely collapse together, and universal behavior is observed in both sets of growth regimes. The second regime corresponds to the branching micelle regime based on the recent Cryo-TEM observations for the branching micelles of $C_{12}E_5$ micellar solutions [14]. In the first growth regime, R_H is related to the molecular weight by a simple power law for a flexible polymer, $R_H \sim M_w^\nu$ [18,19]. The average micelle length is a linear function of molecular weight in the dilute concentration regime due to the one dimensional growth and is also given by [20]

$$M \sim \bar{L} \sim c^\alpha \exp(E_{\text{cap}}/2k_B T). \quad (2)$$

Since $R_H \sim c^{\alpha\nu}$, in the first growth regime $c < c_J$, $\alpha\nu \sim 0.29$ is obtained from the universal behavior of R_H/R_o in Fig. 3(b). From the SLS measurement, we obtained the exponent values of ν , 0.64 ± 0.03 [21]. We can obtain the exponent value of α , scaling as $\bar{L} \sim c^\alpha$, 0.45 ± 0.03 ($c < c_J$), which is in good agreement with the theoretical power law ($\alpha \sim 0.5$) predicted by the Flory-Huggins lattice model for linear micelles. Therefore, for $c < c_J$ the end defect is dominant and a uniaxial micellar growth occurs. However, the micellar growth near the critical point cannot be explained successfully by this growth model due to a long range interaction, which gives a very different power law with exponent $\alpha \sim 1.2$ [22].

For $c > c_J$, it is worthwhile to note that the R_H/R_o follows a universal curve which departs from the simple growth power law. This second growth regime shows the formation of the branched point in previous Cryo-TEM observations [14]. Furthermore, for $c \gg c_J$, R_H decreases as the concentration is increased as shown in Fig. 3. This is similar to the semidilute concentration behavior of living polymer solutions [23].

The general trends of R_H with the concentration can be understood in terms of the number density of topological defects, ρ_z , which scales nonlinearly with the solute volume fraction ϕ [24,25];

$$\rho_z \sim \phi^{z/2} e^{-\epsilon_z} \quad (3)$$

for the end defect (end cap), $z = 1$ and for the junction defect (threefold branching point) $z = 3$. ϵ_1 and ϵ_3 are the end defect and the junction defect, respectively. The values of c_J estimated from η and R_H data are the points where the number densities of cylindrical micelles with free end caps and branching micelles with threefold junctions are approximately the same.

Now, we confront the theoretical prediction with the strong molar ratio dependence of the topological transition points c_J . When c_J is determined at $\rho_1 \approx \rho_3$, the theory indicates that the topological transition occurs at the value of $r = c_o R$ (c_o is the spontaneous curvature and R is the radius of a cylindrical micelle) at r_n with [7,8,26]

$$r_n = \frac{1}{\alpha_3 - \alpha_1} \left[(\beta_1 - \beta_3) + \frac{\bar{\kappa}}{\kappa} - \frac{\gamma_3 - \gamma_1}{4\pi} + \frac{1}{4\pi} \ln \phi_J \right], \quad (4)$$

where ϕ_J ($\sim c_J$) is a volume fraction of solute molecules at a transition point. This theoretical prediction implies that as the spontaneous curvature decreases, ϕ_J decreases as $r_n \sim \ln \phi_J$. This calculation from the familiar Helfrich curvature energy is valid for small curvatures, such as for microemulsions or vesicles. To account for the details of the molecular interaction, the third term on the right-hand side in Eq. (4) is added, so that Eq. (4) gives a reasonable estimation of micelle properties, the bending elasticity of the micelles, their tendency to form defects (end cap and junctions), free energy of the micelles, etc. [6,7,27].

Small amounts of DMPC molecules added into $C_{12}E_5$ micelles decrease spontaneous curvatures of micelles due to their molecular structure [15], leading to the decrease of r , while R remains constant. Then, the value of ϕ_J shifts toward a lower value by adding DMPC (Fig. 4). Equation (4) can be reformulated with the relation of r_n and m [28], as follows:

$$\ln \phi_J = -\frac{1.29(\alpha_3 - \alpha_1)}{10\alpha_1} \left(m - \frac{1}{1.29} \frac{\alpha_1}{\alpha_3} P \right) + Q. \quad (5)$$

This can give us the quantitative prediction of topological transition points as a function of m . The best fitted experimental data with Eq. (5) in Fig. 4 gives us $\alpha_3/\alpha_1 = -0.74 \pm 0.08$, $P \approx -73.2$, and $Q \approx -4.2$ [29]. The value of α_3/α_1 is similar to the theoretical value, ~ -0.9 [7]. This indicates the values of ϕ_J obtained from the DLS and the viscosity measurements are consistent with the topological transition points. The branched micelles form only when the micelles are extremely long, that is, when

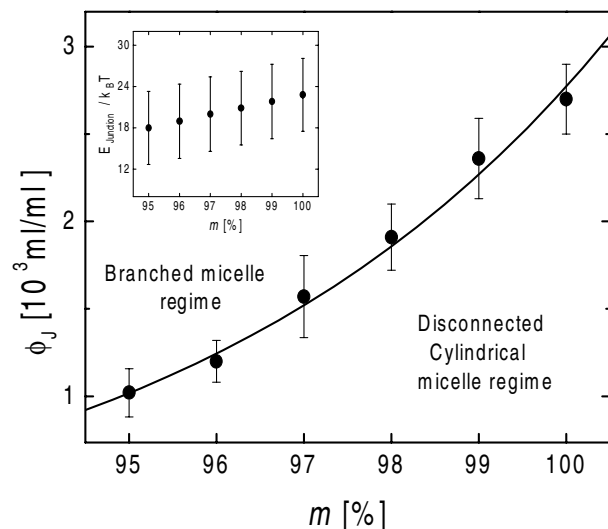


FIG. 4. Topological transition points ϕ_J vs m . The solid line is the theoretical calculation. The inset is the junction-defect energy estimated using Eq. (6).

the micelle solution has less end defects because the local curvature defect energy cost for forming a junction is higher than that for forming a spherical end cap [4,6,7]. The micelles with a lower molar ratio are longer due to their large end-defect energies and have a smaller energy cost ($\Delta\epsilon \equiv \epsilon_3 - \epsilon_1$) for forming junction defects. Then, the micelles with a lower value of m show the topological transition at lower concentrations.

Using these results and the relation of r vs m [26], we estimated the junction-defect energy as a function of m using the equation

$$\epsilon_3 = -1.29 \frac{\alpha_3}{\alpha_1} m + P. \quad (6)$$

The junction-defect energies are shown as an inset in Fig. 4. The pure surfactant micelle ($m = 100$) has the energy difference, $\Delta\epsilon$, with $11.4k_B T$, which is in good agreement with the theoretical prediction, about $10k_B T$ [6]. Junction energies decrease with the amount of DMPC. This is the opposite tendency to the case of the end-defect energy. Any change of conditions which increases the end-defect energy decreases the junction-defect energy simultaneously, since in a junction the curvature change has the opposite sense to that of an end defect due to the bilayer of a junction point [6,7].

In summary, we have shown for the first time that the topological transition of the nonionic micellar solutions ($C_{12}E_5/DMPC/H_2O$) was strongly affected by defect energies and spontaneous curvature. This finding is in good agreement with theoretical calculations [8]. This finding is important for understanding the rheological problems of polymerlike micelle systems, and also obviously for the hierarchical nature of biological systems (e.g., biogel, network of biopolymers, etc.).

This work was supported by a grant from the 2001 Korean National Cancer Program, Ministry of Health & Welfare and from Advanced Backbone IT Technology Development Project (IMT-2000-B3-2), Ministry of Information and Communication. We express our thanks to Professor D. Andelman and Professor P. Pincus for reading the final manuscript.

*Author to whom correspondence should be addressed.
Electronic address: mwkim@kaist.ac.kr

- [1] G. Porte, R. Gomati, O. El Hataimy, J. Appell, and J. Marignan, *J. Phys. Chem.* **90**, 5746 (1986); J. Appell, G. Porte, A. Khatory, F. Kern, and S. J. Candau, *J. Phys. II (France)* **2**, 1045 (1992).
- [2] S. J. Candau, A. Khatory, F. Lequeux, and F. J. Kern, *J. Phys. IV (France)* **3**, 197 (1993).
- [3] F. Lequeux and S. J. Candau, in *Structure and Flow in Surfactant Solutions*, ACS Symposium Series Vol. 578 (ACS, Washington, D.C., 1994).
- [4] T. J. Drye and M. E. Cates, *J. Chem. Phys.* **96**, 1367 (1992).
- [5] Y. Bohbot, A. Ben-Shaul, R. Granek, and W. M. Gelbart, *J. Chem. Phys.* **103**, 8764 (1995).
- [6] S. May, Y. Bohbot, and A. Ben-Shaul, *J. Phys. Chem. B* **101**, 8648 (1997).
- [7] T. Tlusty and S. A. Safran, *J. Phys. Condens. Matter* **12**, A253 (2000).
- [8] T. Tlusty, S. A. Safran, and R. Strey, *Phys. Rev. Lett.* **84**, 1244 (2000).
- [9] P. Pincus, *Science* **290**, 1307 (2000).
- [10] D. Danino, Y. Talmon, H. Levy, G. Beinert, and R. Zana, *Science* **269**, 1420 (1995).
- [11] Z. Lin, *Langmuir* **12**, 1729 (1996).
- [12] R. Oda, P. Panizza, M. Schumtz, and F. Lequeux, *Langmuir* **13**, 6407 (1997).
- [13] A. Bernheim-Groswasser, R. Zana, and Y. Talmon, *J. Phys. Chem. B* **104**, 4005 (2000).
- [14] A. Bernheim-Groswasser, E. Wachtel, and Y. Talmon, *Langmuir* **16**, 4131 (2000).
- [15] S. Y. Kwon and M. W. Kim, *Langmuir* **17**, 8016 (2001).
- [16] F. Lequeux, *Europhys. Lett.* **19**, 675 (1992).
- [17] A. Khatory, F. Kern, F. Lequeux, J. Appell, G. Porte, N. Morie, A. Ott, and W. Urbach, *Langmuir* **9**, 932 (1993).
- [18] P. G. de Gennes, in *Scaling Concepts in Polymer Physics* (Cornell University Press, Ithica, NY, 1976).
- [19] Small angle neutron scattering and SLS give $\bar{L}/l_p > 10$ (l_p is persistence length) for all solutions, which makes it possible to use the power law for a flexible polymer.
- [20] S. Safran, P. Pincus, and M. E. Cates, *J. Phys. (Paris)* **51**, 503 (1990).
- [21] The values of R_H, M_w were determined as a function of temperature 285–291 K, which gives the power law.
- [22] P. Schurtenberger, C. Cavaco, F. Tiberg, and O. Regev, *Langmuir* **12**, 2894 (1996).
- [23] M. E. Cates and S. J. Candau, *J. Phys. Condens. Matter* **2**, 6869 (1990).
- [24] T. J. Drye and M. E. Cates, *J. Chem. Phys.* **96**, 1367 (1992).
- [25] T. Tlusty and S. A. Safran, *Science* **290**, 1328 (2000).
- [26] In [7], $\epsilon_1 = 4\pi\kappa(\alpha_1 r + \beta_1) + \gamma_1\kappa$, $\epsilon_3 = 4\pi\kappa(\alpha_3 r + \beta_3) + \gamma_3\kappa$, where $\alpha_1 < 0$, $\alpha_3 > 0$, $\gamma_1 < 0$, $\gamma_3 > 0$, and κ is a bending modulus, and $\bar{\kappa}$ is a saddle-splay modulus. α and β are the constants for optimal defect structure of micelles. γ is the constant of order unity for the molecular interaction.
- [27] D. R. Fattal, D. Andelman, and A. Ben-Shaul, *Langmuir* **11**, 1154 (1995).
- [28] The end-defect energy ϵ_1 is proportional to r [26], and m is linearly proportional to ϵ_1 , $\epsilon_1 \approx -1.29m + 141$ (in units of $k_B T$) based on experimental data (Fig. 1). If we set $\epsilon_1 \approx 4\pi\kappa(\alpha_1 r + \beta_1) + \gamma_1\kappa \approx -1.29m + 141$, where κ is of order $10k_B T$, this gives a linear relation as $r_n = -1.29/(4\pi\kappa\alpha_1)m + 1/(4\pi\kappa\alpha_1)(141 - 4\pi\kappa\beta_1 - \kappa\gamma_1)$, since two equations for ϵ_1 are valid at $r \approx r_n$.
- [29] P and Q are $(\alpha_3/\alpha_1)(141 - 4\pi\kappa\beta_1 - \kappa\gamma_1) + 4\pi\kappa(\beta_3 + \gamma_3/4\pi)$ and $4\pi[(\alpha_1/\alpha_3)(\beta_3 + \gamma_3/4\pi) - \beta_1 - \bar{\kappa}/\kappa - \gamma_1/4\pi]$, respectively, and have a reasonable order of magnitude compared with the theoretical estimates of $P \sim -75$ and $Q \sim -9$ [6,7].